

Article

Control of Crystalline-Amorphous Structures of Polyhedral Oligomeric Silsesquioxanes Containing Two Types of Ammonium Side-Chain Groups and Their Properties as Protic Ionic Liquids

Ryoya Hasebe and Yoshiro Kaneko *

Graduate School of Science and Engineering, Kagoshima University, 1-21-40 Korimoto, Kagoshima 890-0065, Japan; k7959128@kadai.jp

* Correspondence: ykaneko@eng.kagoshima-u.ac.jp

Academic Editor: Masafumi Unno

Received: 21 November 2019; Accepted: 11 December 2019; Published: 12 December 2019



Abstract: Polyhedral oligomeric silsesquioxanes (POSSs), **Am-POSS(x,y)**, prepared by hydrolytic condensation, contains two types of ammonium side-chain groups, where the numbering of *x* and *y* represents the type of ammonium ions in the POSS structure, corresponding to primary (1), secondary (2), tertiary (3), and quaternary (4) ammonium ions. Mixtures of the two starting materials selected from organotrialkoxysilanes containing primary, secondary, and tertiary amines and a quaternary ammonium salt [(RO)₃Si(CH₂)₃R', R = CH₃ or CH₂CH₃, R' = NH₂, NHCH₃, N(CH₃)₂, and N(CH₃)₃Cl] were dissolved in dimethyl sulfoxide (DMSO). The hydrolytic condensation was performed in the presence of bis(trifluoromethanesulfonyl)imide (HNTf₂) and water. All **Am-POSS(x,y)** structures consisted of a cage-type octamer (T₈-POSS), as confirmed by ²⁹Si NMR spectrometry and matrix-assisted laser desorption ionization-time of flight mass spectrometry (MALDI-TOF MS). Differential scanning calorimetry (DSC) and X-ray diffraction (XRD) analyses indicated that **Am-POSS(1,3)**, **Am-POSS(1,4)**, and **Am-POSS(2,4)** had amorphous structures. These POSSs have two or three differences in the number of methyl groups between the two types of ammonium side-chains. Conversely, **Am-POSS(1,2)**, **Am-POSS(2,3)**, and **Am-POSS(3,4)** had crystalline structures. The difference in the number of methyl groups between the two types of ammonium side-chains in these POSSs is only one. Therefore, the crystalline-amorphous structure of **Am-POSS(x,y)** is controlled by the side-chain group combinations. Furthermore, **Am-POSS(1,3)**, **Am-POSS(1,4)**, and **Am-POSS(2,4)** are protic ionic liquids with relatively low flow temperatures.

Keywords: silsesquioxane; POSS; ionic liquid

1. Introduction

Polyhedral oligomeric silsesquioxanes (POSSs), which are generally prepared by the hydrolytic condensation of trifunctional silane compounds, such as organotrialkoxysilanes and organotrichlorosilanes, have attracted much attention in recent years as compounds having both inorganic and organic characteristics. In addition to the remarkable thermal and chemical stability derived from siloxane-bond frameworks, good dispersibility and solubility are provided due to regulated cage structures and suitable side-chain groups [1–4]. POSSs are, therefore, in great demand as dispersible inorganic compounds for the development of organic–inorganic hybrid materials [5–10].

Well-known POSSs are typically crystalline, cage-type octamers, because of their isotropic cubic structure. The amorphization of POSSs is one of the recent interesting topics in basic research and material applications. For example, amorphous POSS dimers [11] and polymers [12–14] are prepared

by linking a plurality of POSSs, and are applied as transparent thermostable materials. There are some examples of large-sized POSSs (e.g., cage-type decamers) [15,16] and incomplete POSSs [17], which are also amorphous.

As a simple method to amorphize POSSs, we have prepared POSS with randomly arranged two types of ammonium side-chain groups (3-aminopropyl and 3-(2-aminoethylamino)propyl groups protonated with trifluoromethanesulfonic acid (HOTf)) [18]. In addition, it was also found that quaternary ammonium and imidazolium salt-containing POSS is amorphous, having no melting point (T_m) [19]. This POSS had a glass transition point (T_g) of $-8\text{ }^\circ\text{C}$, and the temperature at which it tilted and flowed was $30\text{ }^\circ\text{C}$, showing the property of room temperature ionic liquid (IL).

As mentioned above, amorphous POSSs with randomly arranged two types of side-chain groups exhibited characteristics that are relevant for various material applications. However, no detailed investigation has been performed on how side-chain combinations affect the amorphous or crystalline morphology.

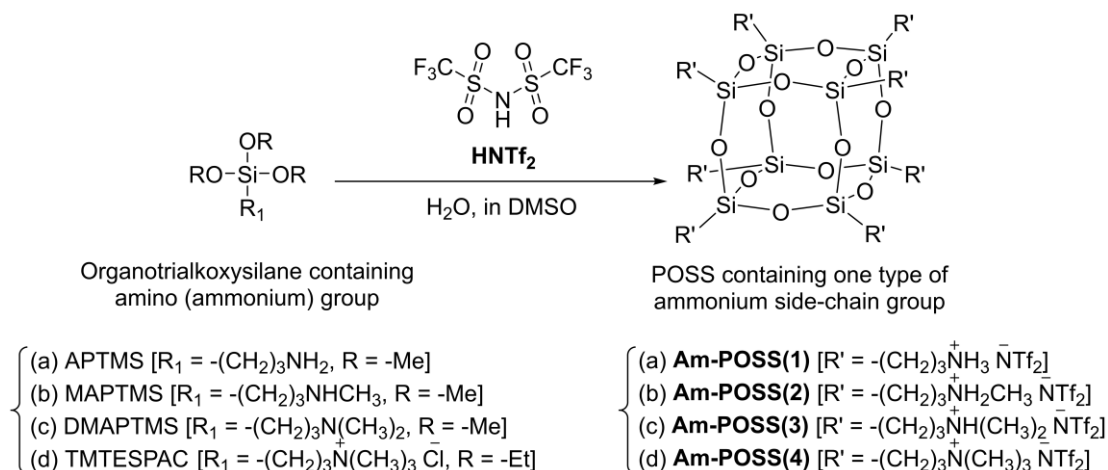
In this study, the effect of combinations of the two side-chains on the crystalline-amorphous structure of the POSSs containing two types of ammonium side-chain groups (**Am-POSS(x,y)**) was investigated, where the numbering of x and y represents the type of ammonium ions in the POSS structure, corresponding to primary (1), secondary (2), tertiary (3), and quaternary (4) ammonium ions. In addition, the properties of **Am-POSS(x,y)** as ionic liquids (ILs) were evaluated.

2. Results and Discussion

2.1. Preparation and Characterization of POSSs Containing One Type of Ammonium Side-Chain Group (**Am-POSS(x)**)

For comparison, prior to the preparation and characterization of **Am-POSS(x,y)**, POSSs containing one type of ammonium side-chain group (**Am-POSS(x)**, where the numbering of x represented the type of ammonium ion in the POSS structure, corresponding to primary (1), secondary (2), tertiary (3), and quaternary (4) ammonium ions) were prepared and characterized. In our previous studies on the preparation of ammonium-functionalized POSSs using superacid catalysts, the solvent water was yielded a mixture of cage-type octamer (main product) and decamer (minor product) [20], while applying the solvent dimethyl sulfoxide (DMSO) selectively provided only a cage-type octamer in higher yield at short reaction times [21]. Therefore, DMSO was used as a solvent in this study.

Am-POSS(x)s were prepared in DMSO by the hydrolytic condensation of 3-aminopropyltrimethoxysilane (APTMS), 3-(methylamino)propyltrimethoxysilane (MAPTMS), 3-(dimethylamino)propyltrimethoxysilane (DMAPTMS), and trimethyl [3-(triethoxysilyl)propyl]ammonium chloride (TMTESPAC), respectively, in the presence of bis(trifluoromethanesulfonyl)imide (HNTf₂) and water (the feed molar ratio of amine:HNTf₂:H₂O was 1.0:1.5:5.0) (Scheme 1). Solubilities of **Am-POSS(x)** are summarized in Table 1. All POSSs were soluble in highly polar organic solvents but insoluble in low polarity organic solvents. POSSs, except **Am-POSS(1)**, was also insoluble in water.



Scheme 1. Preparation of POSSs containing one type of ammonium side-chain group: (a) **Am-POSS(1)**, (b) **Am-POSS(2)**, (c) **Am-POSS(3)**, and (d) **Am-POSS(4)**.

Table 1. The solubility of **Am-POSS(x)**.

Am-POSS(x)	Water	DMSO	DMF	Methanol	Acetone	Acetonitrile	Chloroform	Toluene	<i>n</i> -Hexane
Am-POSS(1)	+	+	+	+	+	+	-	-	-
Am-POSS(2)	-	+	+	+	+	+	-	-	-
Am-POSS(3)	-	+	+	+	+	+	-	-	-
Am-POSS(4)	-	+	+	+	+	+	-	-	-

+: Soluble at room temperature, -: Insoluble at room temperature; DMSO: Dimethyl sulfoxide, DMF: *N,N*-dimethylformamide.

The ¹H NMR spectra of **Am-POSS(x)** in DMSO-*d*₆ showed the signals attributable to the side-chains of the corresponding POSSs (Figure 1). The signals for the methoxy or ethoxy group of the starting materials were not observed (Figure 1), pointing out that the starting materials were not present in the products. The energy-dispersive X-ray (EDX) pattern of **Am-POSS(4)** contained no peaks originating from Cl (*ca.* 2.6 and 2.8 keV). The Si:S atom ratios were estimated to be 1.00:1.95 for **Am-POSS(1)**, 1.00:2.02 for **Am-POSS(2)**, 1.00:1.96 for **Am-POSS(3)**, and 1.00:2.00 for **Am-POSS(4)**, respectively, indicating that the molar ratios of ammonium cations to NTf₂ anions in all products were *ca.* 1:1 (Figure S1).

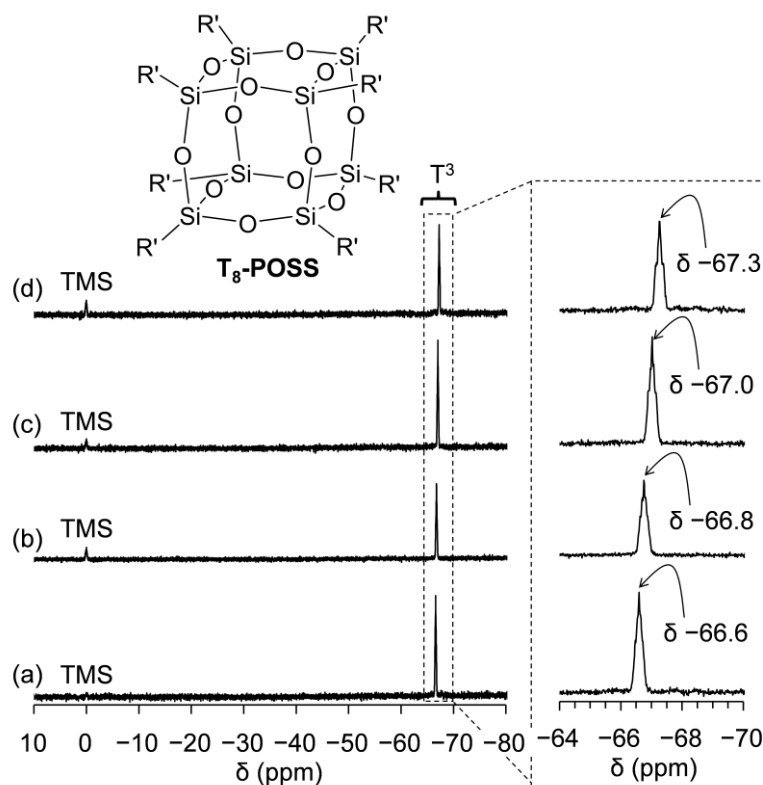


Figure 2. ^{29}Si NMR spectra of (a) **Am-POSS(1)**, (b) **Am-POSS(2)**, (c) **Am-POSS(3)**, and (d) **Am-POSS(4)** in $\text{DMSO-}d_6$ at 40°C . Chemical shifts were referenced to tetramethylsilane (TMS) (δ 0.0).

2.2. Evaluation of Crystalline-Amorphous Structures of **Am-POSS(x)**

The X-ray diffraction (XRD) patterns of all **Am-POSS(x)** showed sharp diffraction peaks, indicating their crystalline structures (Figure 3). In addition, in the differential scanning calorimetry (DSC) curves of **Am-POSS(1)**, **Am-POSS(2)**, **Am-POSS(3)**, and **Am-POSS(4)**, the endothermic peaks due to T_m s were observed at 186 and 209°C (Figure 4a), -1 , 134 , and 180°C (Figure 4b), 94 and 124°C (Figure 4c), and 174°C (Figure 4d), respectively. Multiple endothermic peaks were observed for POSSs, except **Am-POSS(4)**, potentially caused by the different crystalline forms of these POSSs. A more detailed study on the crystalline forms of these POSSs containing one type of ammonium side-chain group is currently in progress.

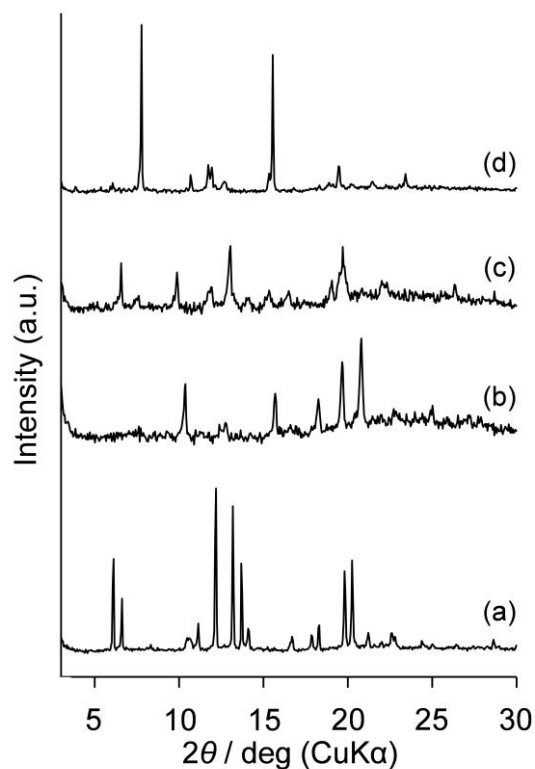


Figure 3. XRD patterns (immediately after preparation) obtained at room temperature (*ca.* 25 °C) of (a) Am-POSS(1), (b) Am-POSS(2), (c) Am-POSS(3), and (d) Am-POSS(4). The amount of each product on the glass was *ca.* 1.0 mg·cm⁻².

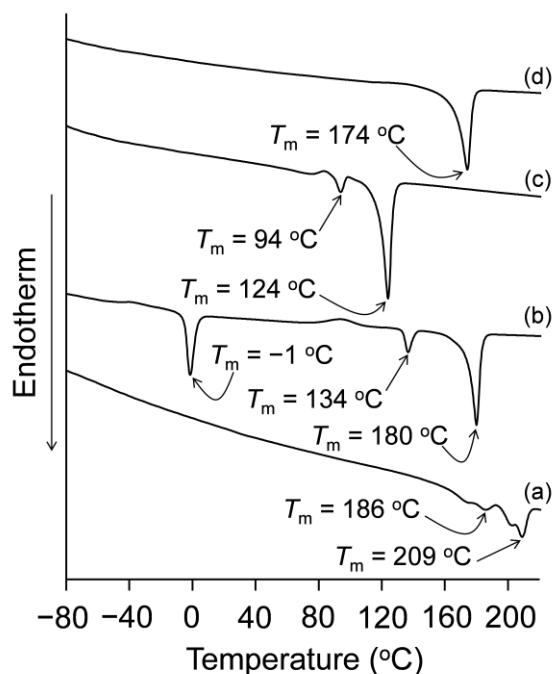
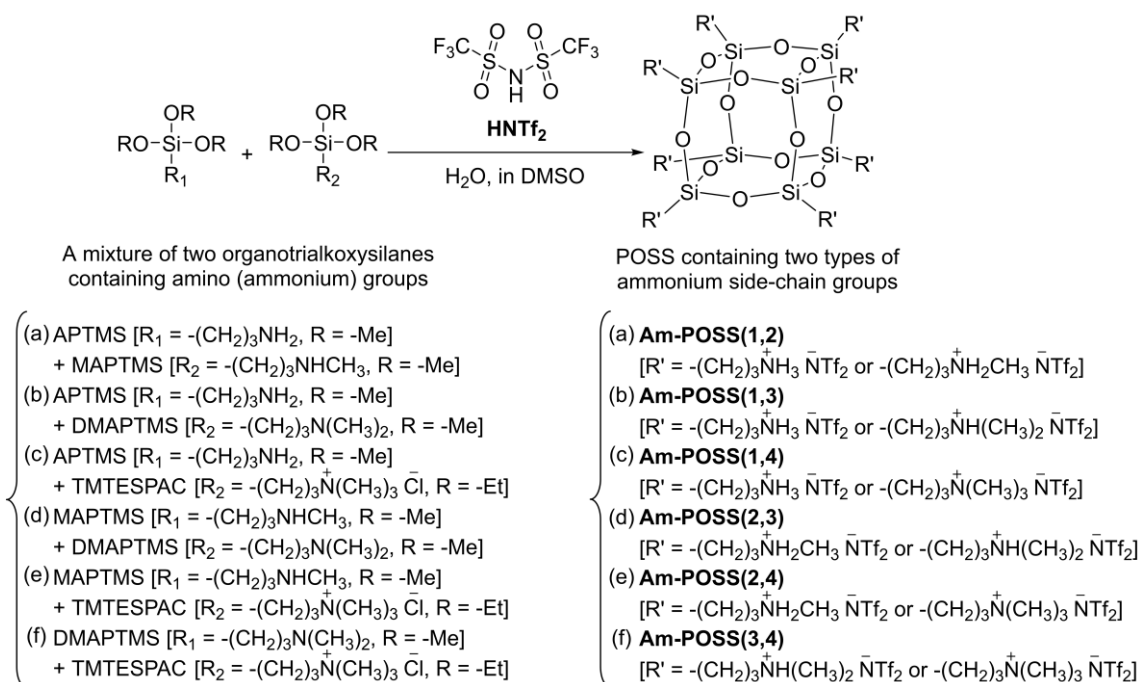


Figure 4. DSC curves of (a) Am-POSS(1), (b) Am-POSS(2), (c) Am-POSS(3), and (d) Am-POSS(4).

2.3. Preparation and Characterization of POSSs Containing Two Types of Ammonium Side-Chain Groups (Am-POSS(*x,y*))

Am-POSS(*x,y*)s were prepared by the hydrolytic condensation of a mixture of two starting materials selected from APTMS, MAPTMS, DMAPTMS, and TMTESPAC. DMSO was used as a solvent together with HNTf₂ and water (the feed molar ratio of amine: HNTf₂:H₂O was 1.0:1.5:5.0) (Scheme 2).

Solubilities of **Am-POSS(x,y)** are summarized in Table 2. All **Am-POSS(x,y)** were soluble in highly polar organic solvents but insoluble in water and low polarity organic solvents.



Scheme 2. Preparation of POSSs containing two types of ammonium side-chain groups: (a) **Am-POSS(1,2)**, (b) **Am-POSS(1,3)**, (c) **Am-POSS(1,4)**, (d) **Am-POSS(2,3)**, (e) **Am-POSS(2,4)**, and (f) **Am-POSS(3,4)**.

Table 2. The solubility of **Am-POSS(x,y)**.

Am-POSS(x,y)	Water	DMSO	DMF	Methanol	Acetone	Acetonitrile	Chloroform	Toluene	n-Hexane
Am-POSS(1,2)	–	+	+	+	+	+	–	–	–
Am-POSS(1,3)	–	+	+	+	+	+	–	–	–
Am-POSS(1,4)	–	+	+	+	+	+	–	–	–
Am-POSS(2,3)	–	+	+	+	+	+	–	–	–
Am-POSS(2,4)	–	+	+	+	+	+	–	–	–
Am-POSS(3,4)	–	+	+	+	+	+	–	–	–

+: Soluble at room temperature, –: Insoluble at room temperature; DMSO: Dimethyl sulfoxide, DMF: *N,N*-dimethylformamide.

The 1H NMR spectra of **Am-POSS(x,y)** in $DMSO-d_6$ showed the signals attributable to the side-chains of both the two selected organotrialkoxysilane components (Figure 5). The signals for the methoxy or ethoxy group of the two starting materials were not observed (Figure 5). The compositional ratio of the two starting material components in **Am-POSS(x,y)** was estimated to be ca. 1:1, considering the integrated ratio of the signals in the 1H NMR spectrum, i.e., $(a + a') : e'$ (4.00:2.96) for **Am-POSS(1,2)**, $(a + a'') : c''$ (4.00:2.01) for **Am-POSS(1,3)**, $c : c'''$ (2.00:2.07) for **Am-POSS(1,4)**, $(a' + a'') : c''$ (4.00:1.99) for **Am-POSS(2,3)**, $c' : c'''$ (2.00:2.00) for **Am-POSS(2,4)**, and $(a'' + a''') : c'''$ (4.00:2.02) for **Am-POSS(3,4)**. The EDX patterns of **Am-POSS(1,4)**, **Am-POSS(2,4)**, and **Am-POSS(3,4)** contained no peaks originating from Cl (ca. 2.6 and 2.8 keV). The Si:S atom ratios were estimated to be 1.00:1.98 for **Am-POSS(1,2)**, 1.00:2.03 for **Am-POSS(1,3)**, 1.00:2.00 for **Am-POSS(1,4)**, 1.00:2.06 for **Am-POSS(2,3)**, 1.00:2.00 for **Am-POSS(2,4)**, and 1.00:1.98 for **Am-POSS(3,4)**, respectively, indicating that the molar ratios of ammonium cations to NTf_2^- anions in all products were ca. 1:1 (Figure S6).

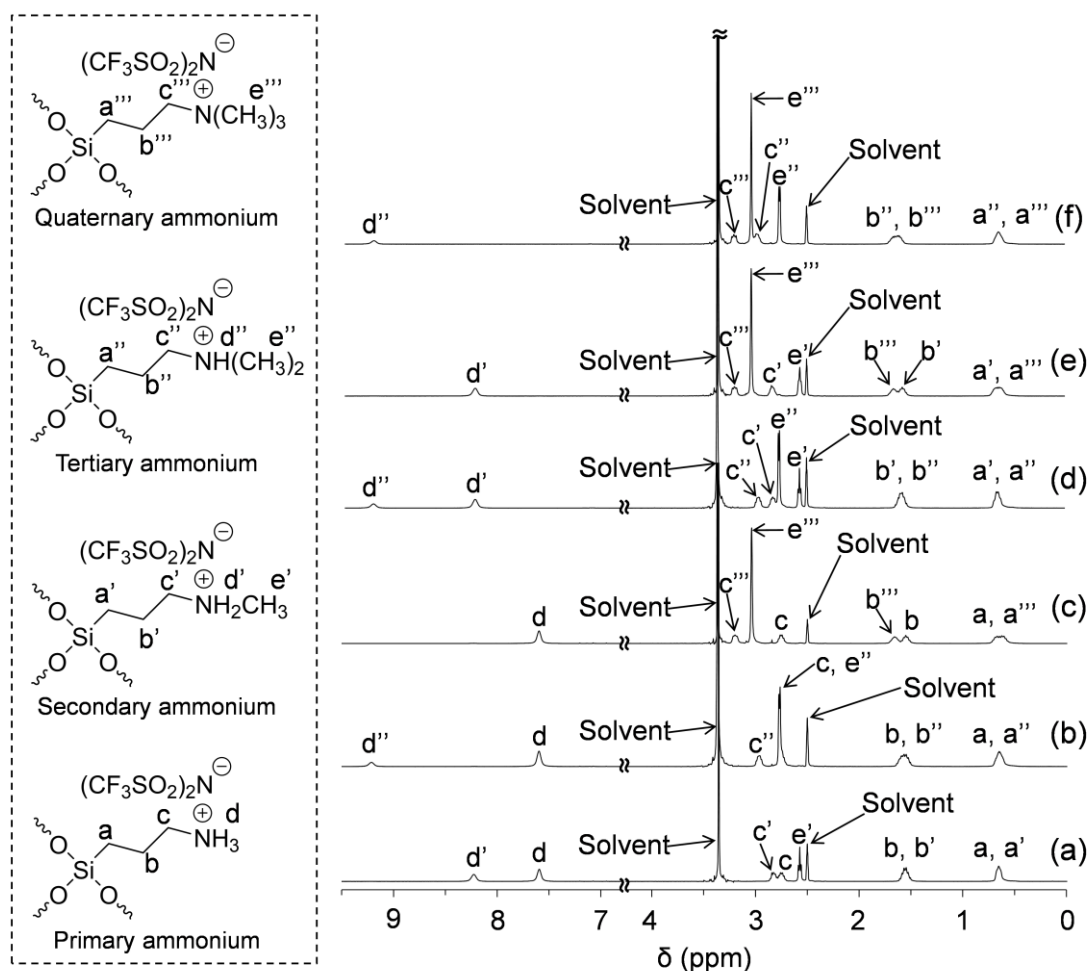


Figure 5. ^1H NMR spectra of (a) Am-POSS(1,2), (b) Am-POSS(1,3), (c) Am-POSS(1,4), (d) Am-POSS(2,3), (e) Am-POSS(2,4), and (f) Am-POSS(3,4) in $\text{DMSO-}d_6$. Chemical shifts were referenced to DMSO (δ 2.5).

The ^{29}Si NMR spectra of Am-POSS(x,y) in $\text{DMSO-}d_6$ at 40°C showed only the sharp signals in the range between δ -66.6 and -67.3 ppm, corresponding to the T^3 structure (Figure 6). These peaks correspond to cage-type octamer (T_8 -POSS). To support these ^{29}Si NMR results, MALDI-TOF MS was performed on these POSSs. The MALDI-TOF MS of all Am-POSS(x,y) showed several peaks ascribed to the masses of T_8 -POSS (Figures S7–S12). In most POSSs, the number of combinations of the two side-chain groups ranged from 1:7 to 7:1. This indicates that the products consisted of T_8 -POSS only, no other POSSs, such as T_{10} - and T_{12} -POSSs were present.

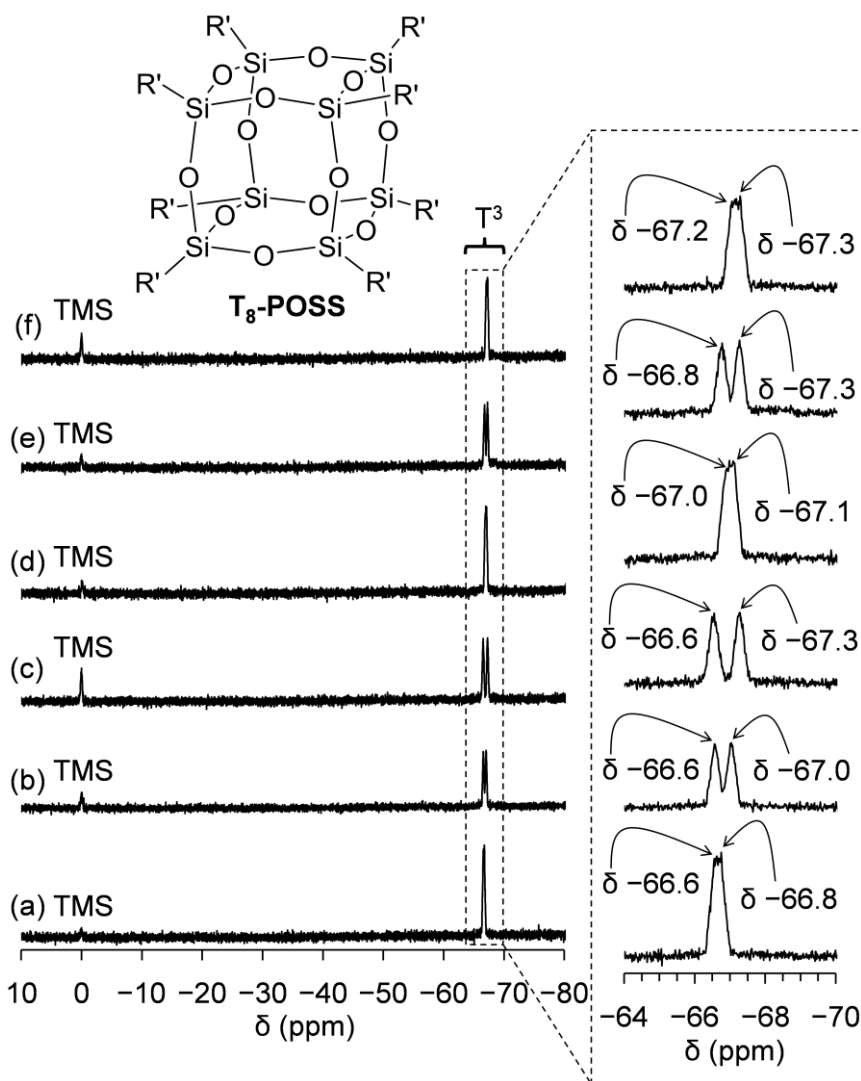


Figure 6. ^{29}Si NMR spectra of (a) Am-POSS(1,2), (b) Am-POSS(1,3), (c) Am-POSS(1,4), (d) Am-POSS(2,3), (e) Am-POSS(2,4), and (f) Am-POSS(3,4) in DMSO- d_6 at 40 °C. Chemical shifts were referenced to tetramethylsilane (TMS) (δ 0.0).

2.4. Evaluation of Crystalline-Amorphous Structures of Am-POSS(x,y)

In the DSC curves of Am-POSS(1,3), Am-POSS(1,4), and Am-POSS(2,4), baseline shifts due to T_g s were observed at -6 °C (Figure 7b, Run 2 in Table 3), 15 °C (Figure 7c, Run 3 in Table 3), and 1 °C (Figure 7e, Run 5 in Table 3), respectively, and endothermic peaks due to T_m s were not observed, suggesting amorphous structures. Conversely, Am-POSS(1,2), Am-POSS(2,3), and Am-POSS(3,4) had T_m s at 154 °C (Figure 7a, Run 1 in Table 3), 104 °C (Figure 7d, Run 4 in Table 3), and 86 and 118 °C (Figure 7f, Run 6 in Table 3), respectively, indicating crystalline structures. In the XRD patterns of these products, immediately recorded after preparation, sharp diffraction peaks were observed only for Am-POSS(1,2) (Figure 8a). Repeating the XRD after more than two weeks resulted in sharp diffraction peaks for Am-POSS(2,3) and Am-POSS(3,4) (Figure 9d,f). Although the crystallization rate was different, Am-POSS(1,2), Am-POSS(2,3), and Am-POSS(3,4) are crystalline compounds. On the other hand, Am-POSS(1,3), Am-POSS(1,4), and Am-POSS(2,4) did not show any diffraction peaks, indicating that these compounds have amorphous structures. These XRD results did support the DSC results.

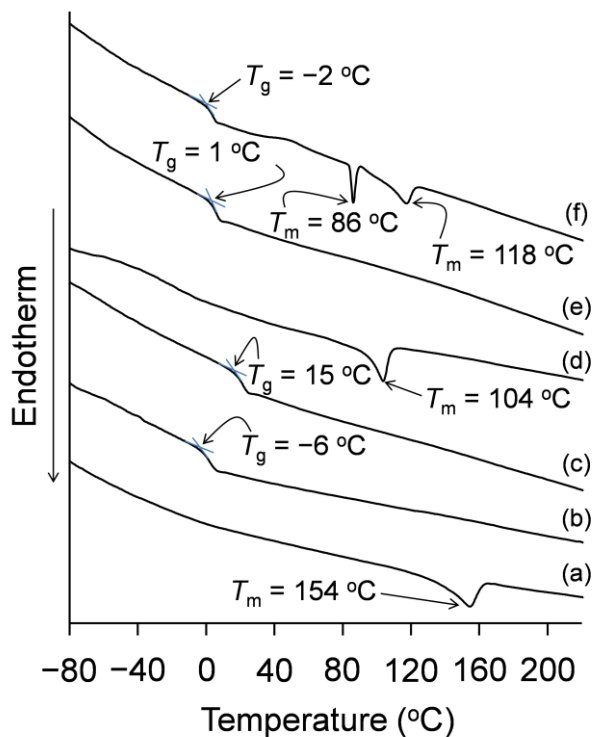


Figure 7. DSC curves of (a) Am-POSS(1,2), (b) Am-POSS(1,3), (c) Am-POSS(1,4), (d) Am-POSS(2,3), (e) Am-POSS(2,4), and (f) Am-POSS(3,4).

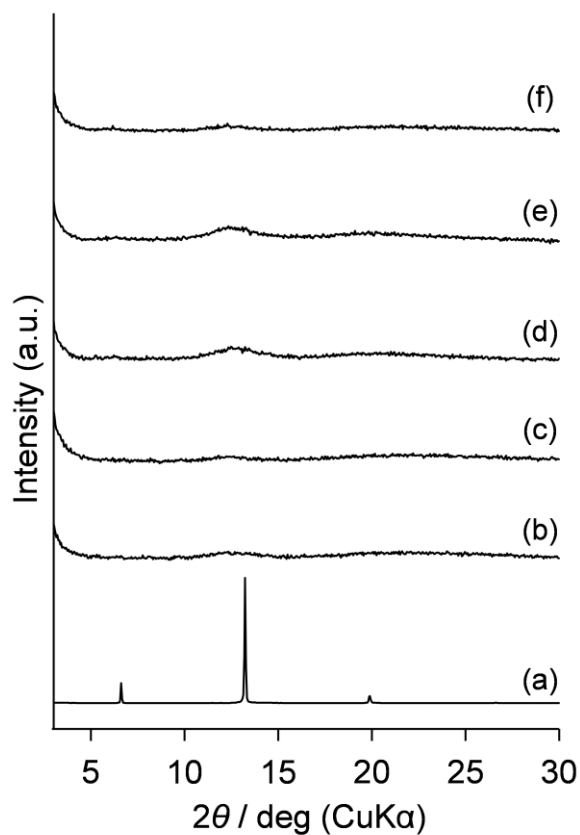


Figure 8. XRD patterns (immediately after preparation) obtained at room temperature (*ca.* 25 °C) of (a) Am-POSS(1,2), (b) Am-POSS(1,3), (c) Am-POSS(1,4), (d) Am-POSS(2,3), (e) Am-POSS(2,4), and (f) Am-POSS(3,4). The amount of each product on the glass was *ca.* 1.0 mg·cm⁻².

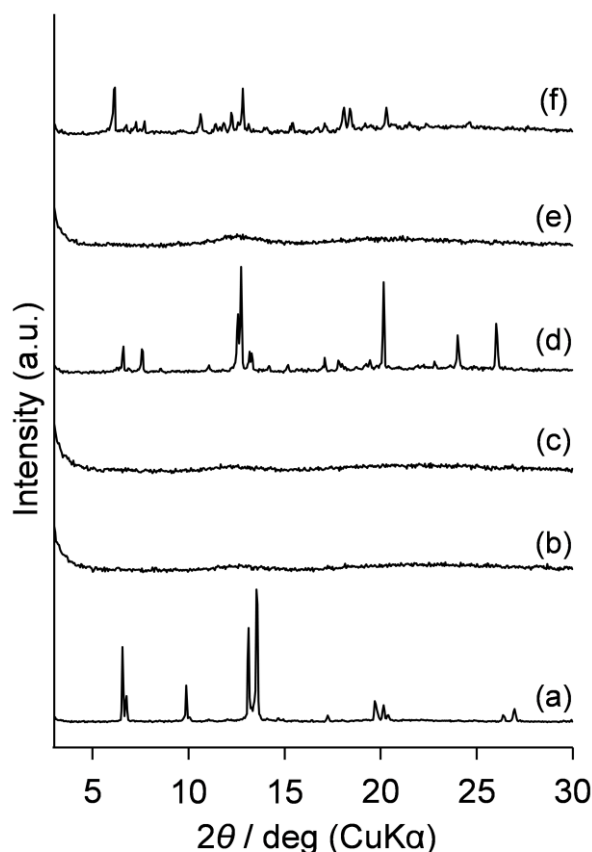


Figure 9. XRD patterns (standing for more than 2 weeks) obtained at room temperature (*ca.* 25 °C) of (a) **Am-POSS(1,2)**, (b) **Am-POSS(1,3)**, (c) **Am-POSS(1,4)**, (d) **Am-POSS(2,3)**, (e) **Am-POSS(2,4)**, and (f) **Am-POSS(3,4)**. The amount of each product on the glass was *ca.* 1.0 mg·cm⁻².

Based on the DSC and XRD results, we concluded that crystalline and amorphous POSSs were selectively prepared, depending on the combination of side-chain groups. **Am-POSS(1,3)**, **Am-POSS(1,4)**, and **Am-POSS(2,4)** have two or three differences in the number of methyl groups between two types of ammonium side-chains. Because of the low molecular symmetry of the POSSs containing two different randomly distributed side-chain groups, crystallization was suppressed, leading to amorphous structures. Conversely, the molecular symmetry of **Am-POSS(1,2)**, **Am-POSS(2,3)**, and **Am-POSS(3,4)** were maintained because of the difference in the numbers of methyl groups between the two types of ammonium side-chains was only one. Therefore, it seems difficult to suppress the crystallization of these POSSs.

2.5. Evaluation of **Am-POSS(x,y)** as ILs

ILs are generally defined as salts that melt below 100 °C (there is also a definition of less than 150 °C). The fundamental thermodynamic properties of ILs have been extensively studied [22–24] for applications, such as green solvents [25–28] and electrolyte materials [29–31]. ILs present unique properties, such as high thermal stability, low vapor pressure, and high ionic conductivity. ILs are classified as aprotic ILs (AILs) or protic ILs (PILs), depending on the absence or presence of active protons. PILs are prepared by a simple neutralization (proton transfer) reaction between a Brønsted acid and a Brønsted base [32,33]. Upon heating, PILs formation can be easily reversed to obtain the original acid and base, showing inferior thermal stability to that of AILs. Therefore, the thermal stability of PILs needs to be improved.

A POSS with IL properties was first developed by Chujo, Tanaka, and co-workers [34]. This POSS contained anionic carboxylate side-chains and imidazolium cations as counterions, and its melting point

(T_m) was 23 °C. Another IL containing a POSS structure was reported by Feng, Zhang, and co-workers. It contained cationic imidazolium side-chains and dodecyl sulfate anions as counterions and had a T_m of 18 °C [35]. We have also reported the preparation of ILs containing randomly structured silsesquioxanes [36,37] and POSS with two types of side-chains [19]. However, all these ILs containing silsesquioxane frameworks were not PILs but AILs.

Although our group reported that cyclic oligosiloxanes containing 3-aminopropyl or 3-(2-aminoethylamino)propyl side-chain groups protonated with HNTf₂ were of PILs nature [38], POSS containing the same side-chain groups did not show IL characteristics, because of the high crystallinity. The amorphous **Am-POSS(1,3)**, **Am-POSS(1,4)**, and **Am-POSS(2,4)** prepared in this study have active protons and showed PILs characteristics.

The flow temperatures of POSSs were confirmed as follows: Samples in glass vessels were maintained in a horizontal position at 200 °C for 15 min, and then cooled to room temperature (*ca.* 25 °C). Next, the vessels were kept horizontally at various temperatures (with 5 °C intervals) for 10 min and then tilted for 15 min. Following this procedure, it was confirmed that **Am-POSS(1,2)**, **Am-POSS(1,3)**, **Am-POSS(1,4)**, **Am-POSS(2,3)**, **Am-POSS(2,4)**, and **Am-POSS(3,4)** flowed at 140 °C (Figure 10a, Run 1 in Table 3), 45 °C (Figure 10b, Run 2 in Table 3), 60 °C (Figure 10c, Run 3 in Table 3), 95 °C (Figure 10d, Run 4 in Table 3), 45 °C (Figure 10e, Run 5 in Table 3), and 95 °C (Figure 10f, Run 6 in Table 3), respectively. These results indicated that amorphous **Am-POSS(1,3)**, **Am-POSS(1,4)**, and **Am-POSS(2,4)** were PILs with relatively low flow temperatures, while crystalline **Am-POSS(1,2)**, **Am-POSS(2,3)**, and **Am-POSS(3,4)** were PILs with relatively high flow temperatures.

Finally, the thermal stabilities of **Am-POSS(x,y)** were investigated by thermogravimetric analyses (TGA) (Figure S13). The pyrolysis temperatures of 5% (T_{d5}) and 10% (T_{d10}) weight losses of **Am-POSS(x,y)** are summarized in Table 3. It was found that the T_{d5} values of all **Am-POSS(x,y)** exceeded 370 °C. These values indicate excellent thermal stabilities and results from the suppression of the molecular tumbling by the silsesquioxane framework [34].

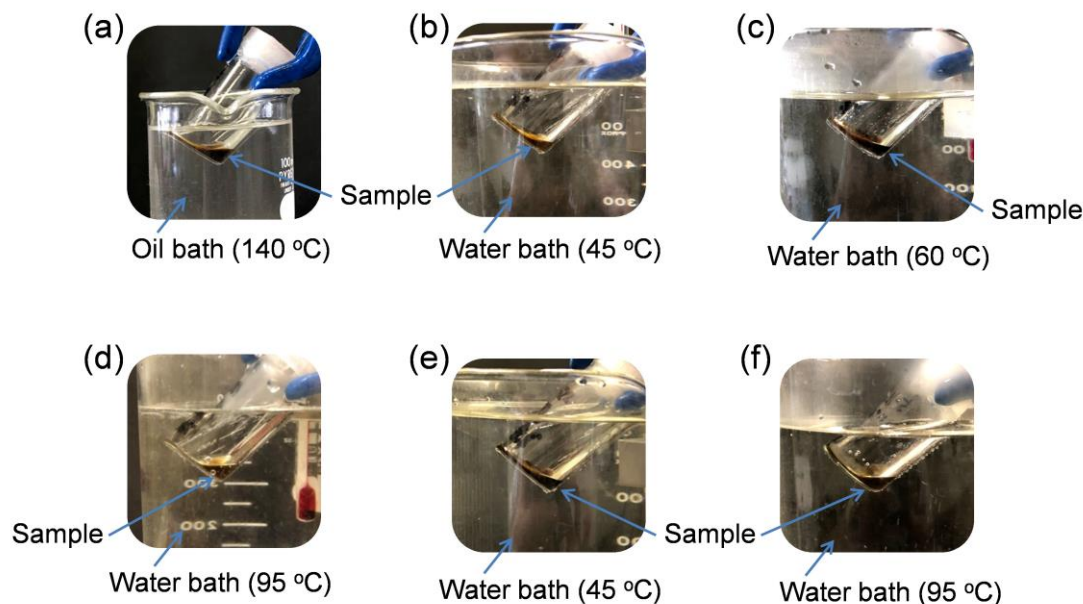


Figure 10. Photographs of flow temperature measurements using (a) **Am-POSS(1,2)**, (b) **Am-POSS(1,3)**, (c) **Am-POSS(1,4)**, (d) **Am-POSS(2,3)**, (e) **Am-POSS(2,4)**, and (f) **Am-POSS(3,4)**.

Table 3. Thermal properties of **Am-POSS(x,y)**.

Run	Am-POSS(x,y)	T _g /°C ^(a)	T _m /°C ^(a)	Flow Temp./°C ^(b)	T _{d5} /°C ^(c)	T _{d10} /°C ^(c)
1	Am-POSS(1,2)	ND ^(d)	154	140	384	397
2	Am-POSS(1,3)	−6	ND ^(d)	45	374	395
3	Am-POSS(1,4)	15	ND ^(d)	60	380	401
4	Am-POSS(2,3)	ND ^(d)	104	95	371	387
5	Am-POSS(2,4)	1	ND ^(d)	45	378	395
6	Am-POSS(3,4)	−2	86,118	95	383	400

(a) Determined as the onset of baseline shift in the curve of 3rd scan by DSC measurement. (b) Determined by visual observation. (c) Determined by TGA. (d) Not detected.

3. Materials and Methods

3.1. Materials

APTMS, MAPTMS, DMAPTMS, TMTESPAC, tris(2,4-pentanedionato)chromium(III) [Cr(acac)₃], and tetramethylsilane (TMS) were purchased from Tokyo Chemical Industry Co., Ltd. (Tokyo, Japan). HNTf₂ was purchased from Kanto Chemical Co., Inc. (Tokyo, Japan). 2,5-Dihydroxybenzoic acid (DHB) was purchased from Bruker Daltonik GmbH (Bremen, Germany). Other reagents and solvents were purchased from FUJIFILM Wako Pure Chemical Co., Ltd. (Osaka, Japan). All reagents and solvents were used without further purification.

3.2. Preparation of **Am-POSS(1)**

A mixture of a 0.5 mol·L^{−1} DMSO solution of HNTf₂ (6.0 mL, 3.0 mmol) and water (0.180 g, 10.0 mmol) was added to APTMS (purity: 96%, 0.374 g, 2.0 mmol) while stirring at room temperature (ca. 25 °C). The resulting solution was further stirred for 2 h. This solution was then heated at ca. 60 °C on a hot plate for 15 h using a disposal tray made of polypropylene (PP), as shown in Figure S14, and the resulting viscous liquid was maintained at 100 °C for 2 h. Subsequently, the crude product was dissolved in methanol (3 mL) at room temperature (ca. 25 °C), and this solution was poured into an acetone-chloroform mixed solvent (1:19 v/v, 180 mL). The insoluble part was isolated by decantation and washed with chloroform (ca. 50 mL, 5 times). To collect the material in a glass container, after dissolving it in methanol, the solution was transferred into a glass container and evaporated. The resulting product was then maintained at 200 °C for 5 h to yield 0.761 g of a white solid product (97% yield based on the ideal chemical formula of one unit of this product, i.e., [SiO_{1.5}(CH₂)₃NH₃ (CF₃SO₂)₂N, FW = 391.4]). ¹H NMR (400 MHz, DMSO-*d*₆): δ 7.75–7.42 (3H, br, −SiCH₂CH₂CH₂NH₃), δ 2.81–2.65 (2H, br, −SiCH₂CH₂CH₂NH₃), δ 1.62–1.40 (2H, br, −SiCH₂CH₂CH₂NH₃), δ 0.65 (2H, t, J = 8.24 Hz, −SiCH₂CH₂CH₂NH₃). ²⁹Si NMR (79.4 MHz, DMSO-*d*₆): δ −66.6 (T³, T₈-POSS).

3.3. Preparation of **Am-POSS(2)**

Am-POSS(2) was prepared similar to **Am-POSS(1)**, except that the starting material was MAPTMS (purity: 95%, 0.407 g, 2.0 mmol). A white solid product (0.679 g) was obtained (84% yield based on the ideal chemical formula of one unit of this product, i.e., [SiO_{1.5}(CH₂)₃NH₂CH₃ (CF₃SO₂)₂N, FW = 405.4]). ¹H NMR (400 MHz, DMSO-*d*₆): δ 8.35–8.09 (2H, br, −SiCH₂CH₂CH₂NH₂CH₃), δ 2.89–2.75 (2H, br, −SiCH₂CH₂CH₂NH₂CH₃), δ 2.57 (3H, t, J = 5.50 Hz, −SiCH₂CH₂CH₂NH₂CH₃), δ 1.65–1.46 (2H, br, −SiCH₂CH₂CH₂NH₂CH₃), δ 0.65 (2H, t, J = 8.24 Hz, −SiCH₂CH₂CH₂NH₂CH₃). ²⁹Si NMR (79.4 MHz, DMSO-*d*₆): δ −66.8 (T³, T₈-POSS).

3.4. Preparation of **Am-POSS(3)**

Am-POSS(3) was prepared similar to **Am-POSS(1)**, except that the starting material was DMAPTMS (purity: 96%, 0.432 g, 2.0 mmol). A white solid product (0.807 g) was obtained (96% yield based on the ideal chemical formula of one unit of this product, i.e., [SiO_{1.5}(CH₂)₃NH(CH₃)₂ (CF₃SO₂)₂N,

FW = 419.4). ^1H NMR (400 MHz, DMSO- d_6): δ 9.37–9.05 (1H, br, $-\text{SiCH}_2\text{CH}_2\text{CH}_2\text{NH}(\text{CH}_3)_2$), δ 3.03–2.90 (2H, br, $-\text{SiCH}_2\text{CH}_2\text{CH}_2\text{NH}(\text{CH}_3)_2$), δ 2.83–2.65 (6H, br, $-\text{SiCH}_2\text{CH}_2\text{CH}_2\text{NH}(\text{CH}_3)_2$), δ 1.71–1.46 (2H, br, $-\text{SiCH}_2\text{CH}_2\text{CH}_2\text{NH}(\text{CH}_3)_2$), δ 0.64 (2H, t, $J = 8.47$ Hz, $-\text{SiCH}_2\text{CH}_2\text{CH}_2\text{NH}(\text{CH}_3)_2$). ^{29}Si NMR (79.4 MHz, DMSO- d_6): δ -67.0 (T^3 , T_8 -POSS).

3.5. Preparation of Am-POSS(4)

Am-POSS(4) was prepared similar to **Am-POSS(1)**, except that the starting material was TMTESPAC (purity: 98%, 0.612 g, 2.0 mmol). A white solid product (0.855 g) was obtained (99% yield based on the ideal chemical formula of one unit of this product, i.e., $[\text{SiO}_{1.5}(\text{CH}_2)_3\text{N}(\text{CH}_3)_3(\text{CF}_3\text{SO}_2)_2\text{N}]$, FW = 433.5). ^1H NMR (400 MHz, DMSO- d_6): δ 3.26–3.15 (2H, br, $-\text{SiCH}_2\text{CH}_2\text{CH}_2\text{N}(\text{CH}_3)_3$), δ 3.03 (9H, s, $-\text{SiCH}_2\text{CH}_2\text{CH}_2\text{N}(\text{CH}_3)_3$), δ 1.76–1.54 (2H, br, $-\text{SiCH}_2\text{CH}_2\text{CH}_2\text{N}(\text{CH}_3)_3$), δ 0.64 (2H, t, $J = 8.47$ Hz, $-\text{SiCH}_2\text{CH}_2\text{CH}_2\text{N}(\text{CH}_3)_3$). ^{29}Si NMR (79.4 MHz, DMSO- d_6): δ -67.3 (T^3 , T_8 -POSS).

3.6. Preparation of Am-POSS(1,2)

Am-POSS(1,2) was prepared similar to **Am-POSS(1)**, except that the starting material was a mixture of APTMS (purity: 96%, 0.187 g, 1.0 mmol) and MAPTMS (purity: 95%, 0.203 g, 1.0 mmol). A white solid product (0.761 g) was obtained (96% yield based on the ideal average chemical formula of one unit of this product, i.e., $\{[\text{SiO}_{1.5}(\text{CH}_2)_3\text{NH}_3(\text{CF}_3\text{SO}_2)_2\text{N}] \times 0.50 + [\text{SiO}_{1.5}(\text{CH}_2)_3\text{NH}_2\text{CH}_3(\text{CF}_3\text{SO}_2)_2\text{N}] \times 0.50 = 398.4$). ^1H NMR (400 MHz, DMSO- d_6): δ 8.34–8.09 (2H, br, $-\text{SiCH}_2\text{CH}_2\text{CH}_2\text{NH}_2\text{CH}_3$ of the MAPTMS component), δ 7.74–7.44 (3H, br, $-\text{SiCH}_2\text{CH}_2\text{CH}_2\text{NH}_3$ of the APTMS component), δ 2.89–2.78 (2H, br, $-\text{SiCH}_2\text{CH}_2\text{CH}_2\text{NH}_2\text{CH}_3$ of the MAPTMS component), δ 2.78–2.68 (2H, br, $-\text{SiCH}_2\text{CH}_2\text{CH}_2\text{NH}_3$ of the APTMS component), δ 2.57 (3H, t, $J = 5.27$ Hz, $-\text{SiCH}_2\text{CH}_2\text{CH}_2\text{NH}_2\text{CH}_3$ of the MAPTMS component), δ 1.68–1.40 (2H, br, $-\text{SiCH}_2\text{CH}_2\text{CH}_2\text{NH}_2\text{CH}_3$ of the MAPTMS component and $-\text{SiCH}_2\text{CH}_2\text{CH}_2\text{NH}_3$ of the APTMS component), δ 0.76–0.47 (2H, br, $-\text{SiCH}_2\text{CH}_2\text{CH}_2\text{NH}_2\text{CH}_3$ of the MAPTMS component and $-\text{SiCH}_2\text{CH}_2\text{CH}_2\text{NH}_3$ of the APTMS component). ^{29}Si NMR (79.4 MHz, DMSO- d_6): δ -66.6 and -66.8 (T^3 , T_8 -POSS).

3.7. Preparation of Am-POSS(1,3)

Am-POSS(1,3) was prepared similar to **Am-POSS(1)**, except that the starting material was a mixture of APTMS (purity: 96%, 0.187 g, 1.0 mmol) and DMAPTMS (purity: 96%, 0.216 g, 1.0 mmol). A brown and viscous solid product (0.804 g) was obtained (99% yield based on the ideal average chemical formula of one unit of this product, i.e., $\{[\text{SiO}_{1.5}(\text{CH}_2)_3\text{NH}_3(\text{CF}_3\text{SO}_2)_2\text{N}] \times 0.50 + [\text{SiO}_{1.5}(\text{CH}_2)_3\text{NH}(\text{CH}_3)_2(\text{CF}_3\text{SO}_2)_2\text{N}] \times 0.50 = 405.4$). ^1H NMR (400 MHz, DMSO- d_6): δ 9.38–9.05 (1H, br, $-\text{SiCH}_2\text{CH}_2\text{CH}_2\text{NH}(\text{CH}_3)_2$ of the DMAPTMS component), δ 7.79–7.40 (3H, br, $-\text{SiCH}_2\text{CH}_2\text{CH}_2\text{NH}_3$ of the APTMS component), δ 3.03–2.90 (2H, br, $-\text{SiCH}_2\text{CH}_2\text{CH}_2\text{NH}(\text{CH}_3)_2$ of the DMAPTMS component), δ 2.83–2.65 (6H, br, $-\text{SiCH}_2\text{CH}_2\text{CH}_2\text{NH}(\text{CH}_3)_2$ of the DMAPTMS component and 2H, br, $-\text{SiCH}_2\text{CH}_2\text{CH}_2\text{NH}_3$ of the APTMS component), δ 1.70–1.41 (2H, br, $-\text{SiCH}_2\text{CH}_2\text{CH}_2\text{NH}(\text{CH}_3)_2$ of the DMAPTMS component and $-\text{SiCH}_2\text{CH}_2\text{CH}_2\text{NH}_3$ of the APTMS component), δ 0.77–0.42 (2H, br, $-\text{SiCH}_2\text{CH}_2\text{CH}_2\text{NH}(\text{CH}_3)_2$ of the DMAPTMS component and $-\text{SiCH}_2\text{CH}_2\text{CH}_2\text{NH}_3$ of the APTMS component). ^{29}Si NMR (79.4 MHz, DMSO- d_6): δ -66.6 and -67.0 (T^3 , T_8 -POSS).

3.8. Preparation of Am-POSS(1,4)

Am-POSS(1,4) was prepared similar to **Am-POSS(1)**, except that the starting material was a mixture of APTMS (purity: 96%, 0.187 g, 1.0 mmol) and TMTESPAC (purity: 98%, 0.306 g, 1.0 mmol). A dark brown and viscous solid product (0.809 g) was obtained (98% yield based on the ideal average chemical formula of one unit of this product, i.e., $\{[\text{SiO}_{1.5}(\text{CH}_2)_3\text{NH}_3(\text{CF}_3\text{SO}_2)_2\text{N}] \times 0.49 + [\text{SiO}_{1.5}(\text{CH}_2)_3\text{N}(\text{CH}_3)_3(\text{CF}_3\text{SO}_2)_2\text{N}] \times 0.51 = 412.9$). ^1H NMR (400 MHz, DMSO- d_6): δ 7.75–7.43 (3H, br, $-\text{SiCH}_2\text{CH}_2\text{CH}_2\text{NH}_3$ of the APTMS component), δ 3.25–3.13 (2H, br,

–SiCH₂CH₂CH₂N(CH₃)₃ of the TMTESPAC component), δ 3.08–2.92 (9H, br, –SiCH₂CH₂CH₂N(CH₃)₃ of the TMTESPAC component), δ 2.81–2.68 (2H, br, –SiCH₂CH₂CH₂NH₃ of the APTMS component), δ 1.78–1.60 (2H, br, –SiCH₂CH₂CH₂N(CH₃)₃ of the TMTESPAC component), δ 1.60–1.42 (2H, br, –SiCH₂CH₂CH₂NH₃ of the APTMS component), δ 0.78–0.44 (2H, br, –SiCH₂CH₂CH₂N(CH₃)₃ of the TMTESPAC component and –SiCH₂CH₂CH₂NH₃ of the APTMS component). ²⁹Si NMR (79.4 MHz, DMSO-*d*₆): δ –66.6 and –67.3 (T³, T₈-POSS).

3.9. Preparation of Am-POSS(2,3)

Am-POSS(2,3) was prepared similar to **Am-POSS(1)**, except that the starting material was a mixture of MAPTMS (purity: 95%, 0.203 g, 1.0 mmol) and DMAPTMS (purity: 96%, 0.216 g, 1.0 mmol). A brown and viscous product (0.779 g) was obtained (94% yield based on the ideal average chemical formula of one unit of this product, i.e., {[SiO_{1.5}(CH₂)₃NH₂CH₃ (CF₃SO₂)₂N, FW = 405.4] × 0.50 + [SiO_{1.5}(CH₂)₃NH(CH₃)₂ (CF₃SO₂)₂N, FW = 419.4] × 0.50 = 412.4). ¹H NMR (400 MHz, DMSO-*d*₆): δ 9.34–9.09 (1H, br, –SiCH₂CH₂CH₂NH(CH₃)₂ of the DMAPTMS component), δ 8.34–8.10 (2H, br, –SiCH₂CH₂CH₂NH₂CH₃ of the MAPTMS component), δ 3.03–2.90 (2H, br, –SiCH₂CH₂CH₂NH(CH₃)₂ of the DMAPTMS component), δ 2.88–2.79 (2H, br, –SiCH₂CH₂CH₂NH₂CH₃ of the MAPTMS component), δ 2.79–2.65 (6H, br, –SiCH₂CH₂CH₂NH(CH₃)₂ of the DMAPTMS component), δ 2.57 (3H, t, J = 5.04 Hz, –SiCH₂CH₂CH₂NH₂CH₃ of the MAPTMS component), δ 1.71–1.39 (2H, br, –SiCH₂CH₂CH₂NH(CH₃)₂ of the DMAPTMS component and –SiCH₂CH₂CH₂NH₂CH₃ of the MAPTMS component), δ 0.75–0.43 (2H, br, –SiCH₂CH₂CH₂NH(CH₃)₂ of the DMAPTMS component and –SiCH₂CH₂CH₂NH₂CH₃ of the MAPTMS component). ²⁹Si NMR (79.4 MHz, DMSO-*d*₆): δ –67.0 and –67.1 (T³, T₈-POSS).

3.10. Preparation of Am-POSS(2,4)

Am-POSS(2,4) was prepared similar to **Am-POSS(1)**, except that the starting material was a mixture of MAPTMS (purity: 95%, 0.203 g, 1.0 mmol) and TMTESPAC (purity: 98%, 0.306 g, 1.0 mmol). A dark brown and viscous product (0.828 g) was obtained (99% yield based on the ideal average chemical formula of one unit of this product, i.e., {[SiO_{1.5}(CH₂)₃NH₂CH₃ (CF₃SO₂)₂N, FW = 405.4] × 0.50 + [SiO_{1.5}(CH₂)₃N(CH₃)₃ (CF₃SO₂)₂N, FW = 433.5] × 0.50 = 419.5). ¹H NMR (400 MHz, DMSO-*d*₆): δ 8.36–8.07 (2H, br, –SiCH₂CH₂CH₂NH₂CH₃ of the MAPTMS component), δ 3.25–3.14 (2H, br, –SiCH₂CH₂CH₂N(CH₃)₃ of the TMTESPAC component), δ 3.10–2.95 (9H, br, –SiCH₂CH₂CH₂N(CH₃)₃ of the TMTESPAC component), δ 2.89–2.77 (2H, br, –SiCH₂CH₂CH₂NH₂CH₃ of the MAPTMS component), δ 2.60–2.53 (3H, br, –SiCH₂CH₂CH₂NH₂CH₃ of the MAPTMS component), δ 1.76–1.60 (2H, br, –SiCH₂CH₂CH₂N(CH₃)₃ of the TMTESPAC component), δ 1.60–1.46 (2H, br, –SiCH₂CH₂CH₂NH₂CH₃ of the MAPTMS component), δ 0.78–0.45 (2H, br, –SiCH₂CH₂CH₂N(CH₃)₃ of the TMTESPAC component and –SiCH₂CH₂CH₂NH₂CH₃ of the MAPTMS component). ²⁹Si NMR (79.4 MHz, DMSO-*d*₆): δ –66.8 and –67.3 (T³, T₈-POSS).

3.11. Preparation of Am-POSS(3,4)

Am-POSS(3,4) was prepared similar to **Am-POSS(1)**, except that the starting material was a mixture of DMAPTMS (purity: 96%, 0.216 g, 1.0 mmol) and TMTESPAC (purity: 98%, 0.306 g, 1.0 mmol). A dark brown and viscous product (0.799 g) was obtained (94% yield based on the ideal average chemical formula of one unit of this product, i.e., {[SiO_{1.5}(CH₂)₃NH(CH₃)₂ (CF₃SO₂)₂N, FW = 419.4] × 0.50 + [SiO_{1.5}(CH₂)₃N(CH₃)₃ (CF₃SO₂)₂N, FW = 433.5] × 0.50 = 426.5). ¹H NMR (400 MHz, DMSO-*d*₆): δ 9.35–9.12 (1H, br, –SiCH₂CH₂CH₂NH(CH₃)₂ of the DMAPTMS component), δ 3.25–3.15 (2H, br, –SiCH₂CH₂CH₂N(CH₃)₃ of the TMTESPAC component), δ 3.09–3.00 (9H, br, –SiCH₂CH₂CH₂N(CH₃)₃ of the TMTESPAC component), δ 3.00–2.91 (2H, br, –SiCH₂CH₂CH₂NH(CH₃)₂ of the DMAPTMS component), δ 2.81–2.68 (6H, br, –SiCH₂CH₂CH₂NH(CH₃)₂ of the DMAPTMS component), δ 1.77–1.47 (2H, br, –SiCH₂CH₂CH₂N(CH₃)₃ of the TMTESPAC component and –SiCH₂CH₂CH₂NH(CH₃)₂ of the DMAPTMS component), δ 0.77–0.44 (2H, br, –SiCH₂CH₂CH₂N(CH₃)₃

of the TMTESPAC component and $-\text{SiCH}_2\text{CH}_2\text{CH}_2\text{NH}(\text{CH}_3)_2$ of the DMAPTMS component). ^{29}Si NMR (79.4 MHz, $\text{DMSO}-d_6$): δ -67.2 and -67.3 (T^3 , T_8 -POSS).

3.12. Measurements

The ^1H and ^{29}Si NMR spectra were recorded using an ECX-400 spectrometer (JEOL RESONANCE Inc., Tokyo, Japan). The absence of Cl and the elemental ratios of Si:S in the products were confirmed by EDX analyses using an XL30 scanning electron microscope (FEI Company, Hillsboro, OR, USA). The MALDI-TOF MS analyses of the products were performed using a Voyager Biospectrometry Workstation Ver. 5.1 (SHIMADZU Corporation, Kyoto, Japan) with 2,5-dihydroxybenzoic acid (DHB) as the matrix under positive ion mode. The DSC analyses were performed on a DSC-60 Plus (SHIMADZU Corporation, Kyoto, Japan). The samples placed in an aluminum capsule were cooled to -140 °C at a rate of 20 °C min^{-1} under a nitrogen flow (300 mL min^{-1}) and then heated from -140 °C to 240 °C at the same rate. The T_g and T_m values were determined as the onset of the baseline shift and as the tops of the endothermic peaks, respectively, in the curves of the third scan (from -140 °C to 240 °C at a rate of 20 °C min^{-1}) to eliminate the heat history in the samples. The XRD patterns were recorded at a scanning speed of $2\theta = 9.0$ ° min^{-1} using an X'Pert Pro diffractometer (PANalytical, Almelo, Netherlands) with Ni-filtered Cu $K\alpha$ radiation (0.15418 nm). The TGA was performed on a TGA-50 (SHIMADZU Corporation, Kyoto, Japan) at a heating rate of 10 °C min^{-1} up to 1000 °C under nitrogen flow (100 mL min^{-1}). The pyrolysis temperatures were determined from the 5% (T_{d5}) and 10% (T_{d10}) weight losses.

4. Conclusions

Am-POSS(x,y) were successfully prepared by the hydrolytic condensation in DMSO of mixtures of two starting materials, which were selected from the organotrialkoxysilanes containing primary, secondary, and tertiary amines and a quaternary ammonium salt, in the presence of HNTf_2 and water. The products consisted of T_8 -POSS only. The DSC curves of **Am-POSS(1,3)**, **Am-POSS(1,4)**, and **Am-POSS(2,4)** did not show the endothermic peaks due to T_m s, indicating their amorphous structures. Conversely, those of **Am-POSS(1,2)**, **Am-POSS(2,3)**, and **Am-POSS(3,4)** showed the endothermic peaks due to T_m s, indicating their crystalline structures. XRD data also supported these results. These results indicate that the crystalline or amorphous structure of **Am-POSS(x,y)** can be controlled by the side-chain group combinations. **Am-POSS(1,3)**, **Am-POSS(1,4)**, and **Am-POSS(2,4)** were PILs with relatively low flow temperatures, while **Am-POSS(1,2)**, **Am-POSS(2,3)**, and **Am-POSS(3,4)** were PILs with relatively high flow temperatures.

Supplementary Materials: The following are available online at <http://www.mdpi.com/1420-3049/24/24/4553/s1>, Figure S1: EDX patterns of **Am-POSS(x)**., Figure S2: MALDI-TOF MS analysis of **Am-POSS(1)**., Figure S3: MALDI-TOF MS analysis of **Am-POSS(2)**., Figure S4: MALDI-TOF MS analysis of **Am-POSS(3)**., Figure S5: MALDI-TOF MS analysis of **Am-POSS(4)**., Figure S6: EDX patterns of **Am-POSS(x,y)**., Figure S7: MALDI-TOF MS analysis of **Am-POSS(1,2)**., Figure S8: MALDI-TOF MS analysis of **Am-POSS(1,3)**., Figure S9: MALDI-TOF MS analysis of **Am-POSS(1,4)**., Figure S10: MALDI-TOF MS analysis of **Am-POSS(2,3)**., Figure S11: MALDI-TOF MS analysis of **Am-POSS(2,4)**., Figure S12: MALDI-TOF MS analysis of **Am-POSS(3,4)**., Figure S13: TGA thermograms of **Am-POSS(x,y)**., Figure S14: Photograph of the apparatus.

Author Contributions: Conceptualization, R.H. and Y.K.; methodology, R.H.; formal analysis, R.H.; investigation, R.H.; resources, Y.K.; data curation, R.H.; writing—original draft preparation, R.H.; writing—review and editing, Y.K.; supervision, Y.K.; project administration, Y.K.; funding acquisition, Y.K.

Funding: This work was supported by JSPS KAKENHI (Grant-in-Aid for Challenging Exploratory Research) Number 15K13711.

Acknowledgments: We acknowledge the support of Y. Suda, M. Wakao, and H. Shinchi of the Graduate School of Science and Engineering, Kagoshima University (Japan) in MALDI-TOF MS measurements.

Conflicts of Interest: The authors declare no conflict of interest.

References

1. Baney, R.H.; Itoh, M.; Sakakibara, A.; Suzuki, T. Silsesquioxanes. *Chem. Rev.* **1995**, *95*, 1409–1430. [[CrossRef](#)]
2. Loy, D.A.; Baugher, B.M.; Baugher, C.R.; Schneider, D.A.; Rahimian, K. Substituent effects on the sol–gel chemistry of organotrialkoxysilanes. *Chem. Mater.* **2000**, *12*, 3624–3632. [[CrossRef](#)]
3. Cordes, D.B.; Lickiss, P.D.; Rataboul, F. Recent developments in the chemistry of cubic polyhedral oligosilsesquioxanes. *Chem. Rev.* **2010**, *110*, 2081–2173. [[CrossRef](#)] [[PubMed](#)]
4. Tanaka, K.; Chujo, Y. Advanced functional materials based on polyhedral oligomeric silsesquioxane (POSS). *J. Mater. Chem.* **2012**, *22*, 1733–1746. [[CrossRef](#)]
5. Feher, F.J.; Wyndham, K.D. Amine and ester-substituted silsesquioxanes: Synthesis, characterization and use as a core for starburst dendrimers. *Chem. Commun.* **1998**, 323–324. [[CrossRef](#)]
6. Naka, K.; Sato, M.; Chujo, Y. Stabilized spherical aggregate of palladium nanoparticles prepared by reduction of palladium acetate in octa(3-aminopropyl)octasilsesquioxane as a rigid template. *Langmuir* **2008**, *24*, 2719–2726. [[CrossRef](#)]
7. Laine, R.M.; Roll, M.F. Polyhedral phenylsilsesquioxanes. *Macromolecules* **2011**, *44*, 1073–1109. [[CrossRef](#)]
8. Kuo, S.W.; Chang, F.C. POSS related polymer nanocomposites. *Prog. Polym. Sci.* **2011**, *36*, 1649–1696. [[CrossRef](#)]
9. Samthong, C.; Laine, R.M.; Somwangthanaroj, A. Synthesis and characterization of organic/inorganic epoxy nanocomposites from poly(aminopropyl/phenyl)silsesquioxanes. *J. Appl. Polym. Sci.* **2013**, *128*, 3601–3608. [[CrossRef](#)]
10. Sharma, A.K.; Sloan, R.; Ramakrishnan, R.; Nazarenko, S.I.; Wiggins, J.S. Structure-property relationships in epoxy hybrid networks based on high mass fraction pendant POSS incorporated at molecular level. *Polymer* **2018**, *139*, 201–212. [[CrossRef](#)]
11. Araki, H.; Naka, K. Syntheses of dumbbell-shaped trifluoropropyl-substituted POSS derivatives linked by simple aliphatic chains and their optical transparent thermoplastic films. *Macromolecules* **2011**, *44*, 6039–6045. [[CrossRef](#)]
12. Araki, H.; Naka, K. Syntheses and properties of star-and dumbbell-shaped POSS derivatives containing isobutyl groups. *Polym. J.* **2012**, *44*, 340–346. [[CrossRef](#)]
13. Maegawa, T.; Irie, Y.; Fueno, H.; Tanaka, K.; Naka, K. Synthesis and polymerization of a *para*-disubstituted T8-caged hexaisobutyl-POSS monomer. *Chem. Lett.* **2014**, *43*, 1532–1534. [[CrossRef](#)]
14. Tokunaga, T.; Koge, S.; Mizumo, T.; Ohshita, J.; Kaneko, Y. Facile preparation of a soluble polymer containing polyhedral oligomeric silsesquioxane units in its main chain. *Polym. Chem.* **2015**, *6*, 3039–3045. [[CrossRef](#)]
15. Chimjarn, S.; Kunthom, R.; Chancharone, P.; Sodkhomkhum, R.; Sangtrirutnugul, P.; Ervithayasuporn, V. Synthesis of aromatic functionalized cage-rearranged silsesquioxanes (T₈, T₁₀, and T₁₂) via nucleophilic substitution reactions. *Dalton Trans.* **2015**, *44*, 916–919. [[CrossRef](#)] [[PubMed](#)]
16. Imai, K.; Kaneko, Y. Preparation of ammonium-functionalized polyhedral oligomeric silsesquioxanes with high proportions of cage-like decamer and their facile separation. *Inorg. Chem.* **2017**, *56*, 4133–4140. [[CrossRef](#)] [[PubMed](#)]
17. Yuasa, S.; Sato, Y.; Imoto, H.; Naka, K. Thermal properties of open-cage silsesquioxanes: The effect of substituents at the corners and opening moieties. *Bull. Chem. Soc. Jpn.* **2019**, *92*, 127–132. [[CrossRef](#)]
18. Tokunaga, T.; Shoiriki, M.; Mizumo, T.; Kaneko, Y. Preparation of low-crystalline POSS containing two types of alkylammonium groups and its optically transparent film. *J. Mater. Chem. C* **2014**, *2*, 2496–2501. [[CrossRef](#)]
19. Harada, A.; Koge, S.; Ohshita, J.; Kaneko, Y. Preparation of a thermally stable room temperature ionic liquid containing cage-like oligosilsesquioxane with two types of side-chain groups. *Bull. Chem. Soc. Jpn.* **2016**, *89*, 1129–1135. [[CrossRef](#)]
20. Kaneko, Y.; Shoiriki, M.; Mizumo, T. Preparation of cage-like octa(3-aminopropyl)silsesquioxane trifluoromethanesulfonate in higher yield with a shorter reaction time. *J. Mater. Chem.* **2012**, *22*, 14475–14478. [[CrossRef](#)]
21. Matsumoto, T.; Kaneko, Y. Selective and high-yielding preparation of ammonium-functionalized cage-like octasilsesquioxanes using superacid catalyst in dimethyl sulfoxide. *Chem. Lett.* **2018**, *47*, 864–867. [[CrossRef](#)]
22. Heintz, A.; Kulikov, D.V.; Verevkin, S.P. Thermodynamic properties of mixtures containing ionic liquids. 1. Activity coefficients at infinite dilution of alkanes, alkenes, and alkylbenzenes in 4-methyl-*n*-butylpyridinium tetrafluoroborate using gas–liquid chromatography. *J. Chem. Eng. Data* **2001**, *46*, 1526–1529. [[CrossRef](#)]

23. Heintz, A.; Kulikov, D.V.; Verevkin, S.P. Thermodynamic properties of mixtures containing ionic liquids. Activity coefficients at infinite dilution of polar solutes in 4-methyl-*N*-butyl-pyridinium tetrafluoroborate using gas–liquid chromatography. *J. Chem. Thermodyn.* **2002**, *34*, 1341–1347. [[CrossRef](#)]
24. Emel'yanenko, V.N.; Verevkin, S.P.; Heintz, A. The gaseous enthalpy of formation of the ionic liquid 1-butyl-3-methylimidazolium dicyanamide from combustion calorimetry, vapor pressure measurements, and ab initio calculations. *J. Am. Chem. Soc.* **2007**, *129*, 3930–3937. [[CrossRef](#)]
25. Welton, T. Room-temperature ionic liquids. Solvents for synthesis and catalysis. *Chem. Rev.* **1999**, *99*, 2071–2083. [[CrossRef](#)]
26. Hallett, J.P.; Welton, T. Room-temperature ionic liquids: Solvents for synthesis and catalysis. 2. *Chem. Rev.* **2011**, *111*, 3508–3576. [[CrossRef](#)]
27. Huddleston, J.G.; Willauer, H.D.; Swatoski, R.P.; Visser, A.E.; Rogers, R.D. Room temperature ionic liquids as novel media for 'clean' liquid–liquid extraction. *Chem. Commun.* **1998**, 1765–1766. [[CrossRef](#)]
28. Dzyuba, S.V.; Bartsch, R.A. Recent advances in applications of room-temperature ionic liquid/supercritical CO₂ systems. *Angew. Chem. Int. Ed.* **2003**, *42*, 148–150. [[CrossRef](#)]
29. Armand, M.; Endres, F.; MacFarlane, D.R.; Ohno, H.; Scrosati, B. Ionic-liquid materials for the electrochemical challenges of the future. *Nat. Mater.* **2009**, *8*, 621–629. [[CrossRef](#)]
30. Ganapatibhotla, L.V.N.R.; Zheng, J.; Roy, D.; Krishnan, S. PEGylated imidazolium ionic liquid electrolytes: Thermophysical and electrochemical properties. *Chem. Mater.* **2010**, *22*, 6347–6360. [[CrossRef](#)]
31. Tsurumaki, A.; Kagimoto, J.; Ohno, H. Properties of polymer electrolytes composed of poly(ethylene oxide) and ionic liquids according to hard and soft acids and bases theory. *Polym. Adv. Technol.* **2011**, *22*, 1223–1228. [[CrossRef](#)]
32. Greaves, T.L.; Drummond, C.J. Protic ionic liquids: Properties and applications. *Chem. Rev.* **2008**, *108*, 206–237. [[CrossRef](#)] [[PubMed](#)]
33. Greaves, T.L.; Drummond, C.J. Protic ionic liquids: Evolving structure–property relationships and expanding applications. *Chem. Rev.* **2015**, *115*, 11379–11448. [[CrossRef](#)] [[PubMed](#)]
34. Tanaka, K.; Ishiguro, F.; Chujo, Y. POSS ionic liquid. *J. Am. Chem. Soc.* **2010**, *132*, 17649–17651. [[CrossRef](#)] [[PubMed](#)]
35. Tan, J.; Ma, D.; Sun, X.; Feng, S.; Zhang, C. Synthesis and characterization of an octaimidazolium-based polyhedral oligomeric silsesquioxanes ionic liquid by an ion-exchange reaction. *Dalton Trans.* **2013**, *42*, 4337–4339. [[CrossRef](#)] [[PubMed](#)]
36. Ishii, T.; Mizumo, T.; Kaneko, Y. Facile preparation of ionic liquid containing silsesquioxane framework. *Bull. Chem. Soc. Jpn.* **2014**, *87*, 155–159. [[CrossRef](#)]
37. Ishii, T.; Enoki, T.; Mizumo, T.; Ohshita, J.; Kaneko, Y. Preparation of imidazolium-type ionic liquids containing silsesquioxane frameworks and their thermal and ion-conductive properties. *RSC Adv.* **2015**, *5*, 15226–15232. [[CrossRef](#)]
38. Hirohara, T.; Kai, T.; Ohshita, J.; Kaneko, Y. Preparation of protic ionic liquids containing cyclic oligosiloxane frameworks. *RSC Adv.* **2017**, *7*, 10575–10582. [[CrossRef](#)]

Sample Availability: Samples of the compounds may be available from the authors.



© 2019 by the authors. Licensee MDPI, Basel, Switzerland. This article is an open access article distributed under the terms and conditions of the Creative Commons Attribution (CC BY) license (<http://creativecommons.org/licenses/by/4.0/>).